

MAPPER: HIGH THROUGHPUT MASKLESS LITHOGRAPHY

E. Slot, M.J. Wieland, G. de Boer, P. Kruit*, G.F. ten Berge, A.M.C. Houkes, R. Jager, T. van de Peut, J.J.M. Peijster, S.W.H.K. Steenbrink, T.F. Teepen, A.H.V. van Veen, B.J. Kampherbeek

MAPPER Lithography B.V., Computerlaan 15, 2628 XK Delft, The Netherlands

*Delft University of Technology, Lorentzweg 1, 2628 CJ, The Netherlands

E-mail address: erwin.slot@mapperlithography.com

ABSTRACT

MAPPER Lithography is developing a maskless lithography technology. The technology combines massively-parallel electron-beam writing with high speed optical data transport used in the telecommunication industry. The electron optics generates 13,000 electron beams that are focused on the wafer by electrostatic lens arrays which are manufactured by using MEMS manufacturing techniques. Each beam has its own optical column to avoid a central cross-over. This secures high throughput (> 10 wafers per hour) at high resolution (< 45 nm half pitch). The 13,000 e-beams are generated by splitting up a single electron beam that originates from a single electron source and are finally accelerated to 5 kV to expose the resist on the wafer. The e-beams are arranged in such a way that they form a rectangular slit with a width of 26 mm, the same width of a field in an optical stepper. During exposure the e-beams are deflected over 2 μ m perpendicular to the wafer stage movement. This means that with one scan of the wafer a full field of 26 mm x 33 mm can be exposed. During the simultaneous scanning of the wafer and deflection of the electron beams the beams are switched on and off by 13,000 light signals, one for each e-beam. The light beams are generated in a data system that contains the chip patterns in a bitmap format. This bitmap is divided over 13,000 data channels and streamed to the e-beams at 1-10 GHz. This paper will explain the design drivers behind the system and provide more detail on the current design. Finally, results of our technology Demonstrator are presented, showing the viability of MAPPER's concept.

Keywords: Massively parallel electron beam lithography, maskless lithography, beam uniformity, high throughput, MAPPER, Demonstrator results, Proof of Concept

1. INTRODUCTION

Since 2002 there has been a renewed interest in massively parallel electron beam lithography for manufacturing of integrated circuits. New manufacturing methods, i.e. MEMS manufacturing, open the possibility to fabricate machines with more than one electron beam. This is required, because due to Coulomb interactions there is a maximum allowable current per electron beam provided a certain resolution and therefore have limited productivity.

Based on MEMS manufacturing methods MAPPER Lithography has designed a massively parallel electron beam machine with 13,000 electron beams. All of the beams can be individually switched on and off. This article will explain the design and the drivers behind it. Next to that MAPPER has built a technology demonstrator with 110 parallel electron beams. This demonstrator has all the functionality to show feasibility of the MAPPER concept. This proof of lithography has been realized in 2007 and this article will show the results.

2. THE MAPPER CONCEPT

For electron beam lithography systems throughput is the challenge. It is well known that very high resolutions can be obtained. Images in resist of 10 nm have been demonstrated^[1] and with alternative techniques resolutions down to 3 nm have been demonstrated^[2]. In additional commercially available STEM microscopes can make probe sizes down to 0.1 nm. However in all these systems the main challenge is to keep the throughput up. To be able to explain the MAPPER concept, requirements for 45 nm half pitch are used from the ITRS roadmap^[3]. Furthermore the targeted throughput is ten, 300mm wafers per hour.

2.1 Required beam current and implications

Since throughput is the main challenge the choice is made to operate the machine in a shot noise limited regime. Provided that 10 % (3σ) total dose variation can be allowed it is decided to allow a budget of 5% (3σ) for shot noise^[4]. Provided poisson statistics 5% (3σ) means that 4000 electrons have to be deposited per pixel or in this case $45 \times 45 \text{ nm}^2$. This comes down to a dose of $30 \mu\text{C}/\text{cm}^2$. To calculate the overall current 69 ($26 \text{ mm} \times 33 \text{ mm}$) fields on the wafer are assumed and a double (redundancy) scan in case some beams fail. For 15 wafers per hour, a current of $150 \mu\text{A}$ on the wafer is required (overhead time not included).

$150 \mu\text{A}$ is a very large current for an e-beam system. For comparison a typical beam current in a SEM is 15 nA . Furthermore for 45 nm resolution the typical maximum current is $0.2 \mu\text{A}$ ^[5]. This means that a system must be designed where the total current is divided over multiple beams with a maximum current of $0.2 \mu\text{A}$.

The overlay budget as can be seen from the ITRS is 8 nm . When $150 \mu\text{A}$ is required on the wafer the total power deposited on the wafer is the product of the current and the acceleration voltage, i.e. 0.75 W for 5 kV and 15 W for 100 kV . To be able to meet the overlay requirements a low acceleration voltage has been chosen, i.e. 5 kV . For more information see Ref. ^[6].

2.2 Electron source and required number of beams

There has been renewed research into different electron emitters and emitter arrays^[7]. However today the only emitter type that is sufficiently stable (i.e. $< 1\%$ current variation over time) for lithography applications is a (single) thermal emitter.

For high throughput in a multi-beam lithography system two aspects of the electron source are important:

1. The total current that is emitted from the source. This must be more than the required $150 \mu\text{A}$ multiplied by the loss factor in the electron optics column
2. The (reduced) brightness of the source. This must be as high as possible to maximize the current per electron beam and thus to maximize the overall throughput

There are several types of thermal emitters available. One has a reduced brightness of $10^6 \text{ A}/\text{cm}^2\text{SrV}$ ^[8] and is the source MAPPER uses in its technology demonstrator. Another option is a LAD-Scandate cathode^[9] and this source has a potential brightness of $10^7 \text{ A}/\text{cm}^2\text{Sr V}$.

If one combines a brightness of $10^7 \text{ A}/\text{cm}^2\text{SrV}$ with the required total current of $150 \mu\text{A}$ it can be calculated that 13,000 electron beams are required with a 12 nA beam current in a total spot size of 31 nm .

2.3 Required data rates and electron beam switching mechanism

To calculate the data rate that is required to switch the 13,000 electron beams the size of one field on the wafer is used: $26 \text{ mm} \times 33 \text{ mm}$. For reasons of dose control for edge placement and CDu the choice has been made to be able to have 20×20 pixels per CD element. For a CD of 45 nm this means 400 pixels of 2.25 nm per CD element. Then the total amount of pixels per field is 1.7×10^{14} . From 2.1 it follows that the time it takes to expose one field is 1.7 s . Therefore the total data rate is 10^{14} pixels per second. If this is divided over the 13,000 electron beams a data rate of 7.6 Gpixels per second per electron beam.

Streaming this amount of data over tens of meters with the transfer rates as calculated can only be done by using optical data transport mechanisms. Therefore the switching mechanism to switch the electron beams on and off is an optical switch as will be explained below.

2.4 Writing strategy

The 13,000 electron beams are arranged in an Electron Optics slit as shown in Figure 1. The beams are on a pitch of $150 \mu\text{m}$ in such a way that if one looks at the beams from the direction perpendicular to where the slit has a width of 26 mm , the beams are effectively $2 \mu\text{m}$ apart. The writing strategy is such that complete fields are exposed within one

stage scan. As one can see from Figure 1 and Figure 2 the wafer is moved underneath the EO slit from one end of the wafer to the other end, this is done by a wafer stage. In the mean time all electron beams are deflected over 2 μm by means of an electrostatic deflector array and the beams are individually switched on and off. In this way a full field can be exposed with only one stage scan.

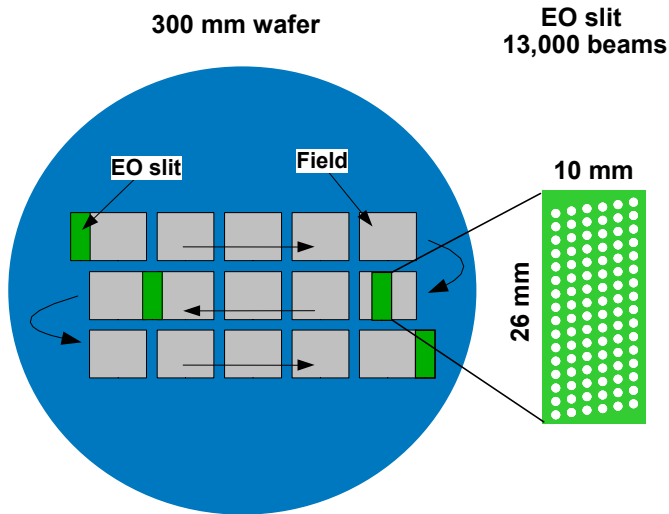


Figure 1. Arrangement of electron beams and writing strategy

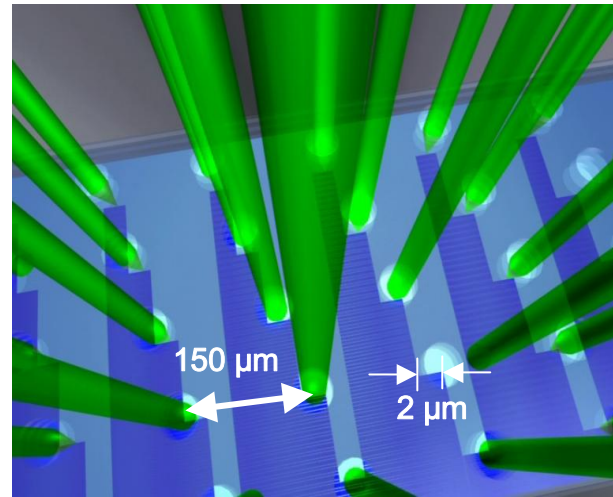


Figure 2. Zoom of (top view of) beam positions in EO slit

2.5 Electron optics configuration

The optics that is required to create an array of focused spots as shown in Figure 1, is shown in Figure 3.

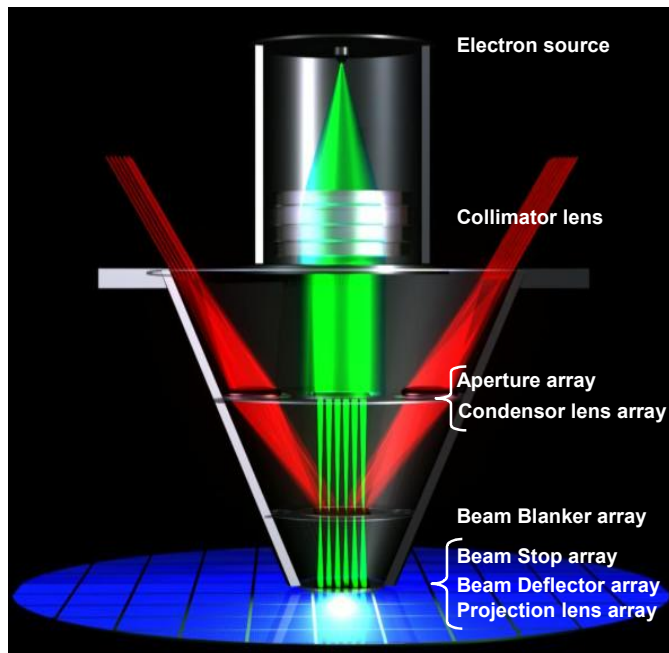


Figure 3. Schematic overview of the electron optics column



Figure 4. Photograph of one of the Demonstrators electron optics columns

It consists of a single high brightness cathode run in space charge limit. An electrostatic collimator lens is used to create a collimated beam. After the collimator the single beam is split up into 13,000 beams by the aperture array. After the aperture array the beamlets are focused by the condenser lens array in the intermediate focus plane. In this plane the beam blaker array is placed that can deflect each individual beam away from a clear aperture on the beam stop array to stop the electrons and switch off the beam at the wafer. After the beam stop array the beams are demagnified by the projection lens array and focused in the wafer plane. A deflector array is positioned between the beam stop array and the projection lens array to scan the beams over a range of 2 μm perpendicular to the wafer stage movement at a frequency of 6 MHz with a positioning accuracy of 1 nm.

2.6 Working principle of the beam blaker array

Figure 5 to Figure 7 explain the working principle of the beam switching mechanism. Every electron beam has its own light signal to switch it on/off. In Figure 5 it is shown that in the

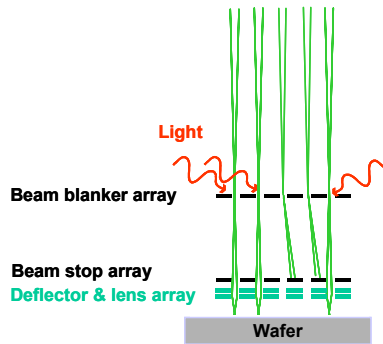


Figure 5. Schematic of 'beam on'/'beam off' states

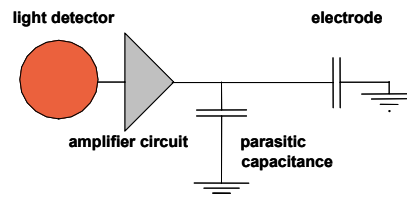


Figure 6. Beam switching mechanism for one electron beam



Figure 7. Optical microscope picture of real beam blaker array

'light off' state the electrons pass through the beam blaker array, but they are deflected to the side and stopped on the beam stop array. In the 'light on' state the electrons pass through the beam blaker array without being deflected and go through the beam stop array and reach the wafer plane.

Figure 6 shows the working principle to switch one electron beam on / off. In the 'light off' situation there is a voltage over the electrode. The electrons pass through the electrode and are deflected. In case light hits the light detector, a PIN photodiode, this removes the voltage over the electrodes and the electrons can pass without being deflected.

The array of electronic circuits has been manufactured in a CMOS process with an integrated photodiode. After that MAPPER has used a dry etch process to etch holes in between the electrodes through the wafer. A picture taken under an optical microscope is shown in Figure 7.

3. RESULTS WITH TECHNOLOGY DEMONSTRATOR

MAPPER has built a 110 electron beam technology Demonstrator based on the concept described in chapter 2. The major difference with respect to the concept description is that the wafer was not scanned underneath the electron beams. Instead, an additional deflector was implemented to substitute for this.

In section 3.1, the first results of a fully functional electron optics column are presented, which proofs our concept. In section 3.2, resist exposure results are presented of an electron optics column to show its performance.

3.1 Proof of Concept in the Demonstrator

The technology Demonstrator is used to demonstrate a fully functional multi-beam electron optics column. A picture of such a column is show in Figure 4. We have used resist exposures to show the functionality of the column. The resist

exposures are done on a target with a Si substrate of $15 \times 15 \text{ mm}^2$ glued onto it. Subsequently, the target is spun with resist. We have used a 40 nm HSQ layer directly on the Si substrate.

The target is pressed against the bottom of the electron optics column, i.e. the projection lens. The Si substrate is in the focal plane of the projection lens, by virtue of the mechanical tolerances of the projection lens and the target.

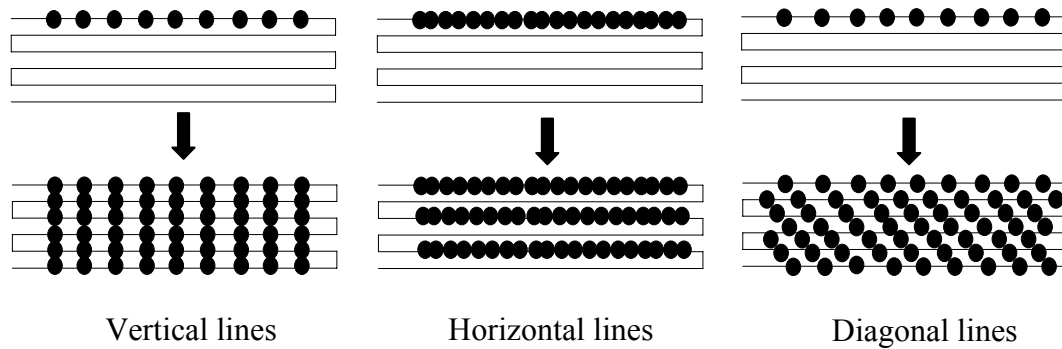


Figure 8. MAPPER writing schematic.

For this technology demonstration, each beamlet is assigned either a horizontal, vertical or diagonal 45 nm dense lines pattern. These patterns are written simultaneously in resist, each beamlet individually controlled by optically switching the blanker array. Figure 8 shows the writing strategy used. The beamlets are scanned across the Si substrate with an X- and Y-deflector, while each beamlet is individually switched on and off at the right time to create either a vertical, horizontal or diagonal lines pattern in resist.

Figure 9 shows a SEM image of a horizontal dense lines pattern written by a single beamlet. Similar images, which are $150 \mu\text{m}$ apart on the Si substrate, are made for each beamlet. A $1 \times 1 \mu\text{m}^2$ is cropped from each image and placed on a hexagonal grid, shown in Figure 10. We identified 72 beamlets that show 45 nm dense lines patterns. The Si substrate was exposed by only 99 beamlets due to column alignment, of which 25 beamlets suffered from defocus due to end-of-array effects and 2 beamlets suffered from a broken optical fiber to the blanker array. This demonstration proves the viability of MAPPER’s multi-beam electron optics concept, described in chapter 2.

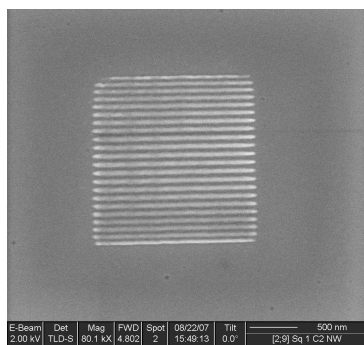


Figure 9. 45 nm Dense Lines pattern of a single beamlet

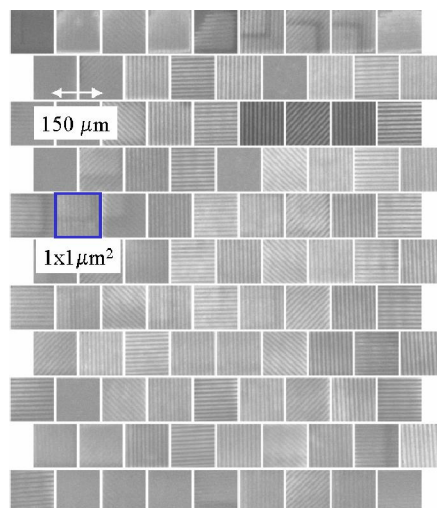


Figure 10. The patterns of each individual beamlet placed on a hexagonal grid

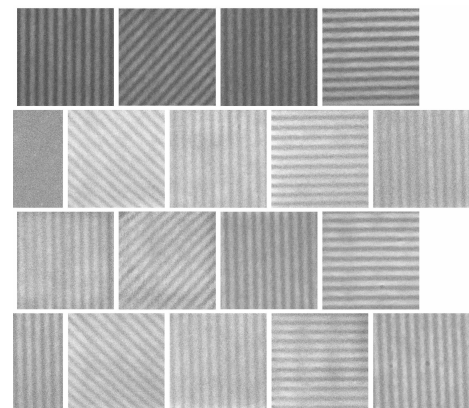


Figure 11. Zoom in of Figure 10. Horizontal, Vertical and Diagonal Lines assigned to each beam individually

3.2 Critical Dimension Uniformity Analysis on 40 nm Dense Lines

The next step is to show the performance of the electron optics column using resist exposures. One of the key performance issues is beam-to-beam Critical Dimension Uniformity (CDu). The spot size on the wafer and the current of each beamlet should be the same. We measure the uniformity by determining the line widths of dense lines patterns for each beamlet.

Analysis method for determining line width variation.

The analysis of the SEM images taken for each beamlet is described. The intensity profile is determined with rulers placed perpendicular to the length of the line.

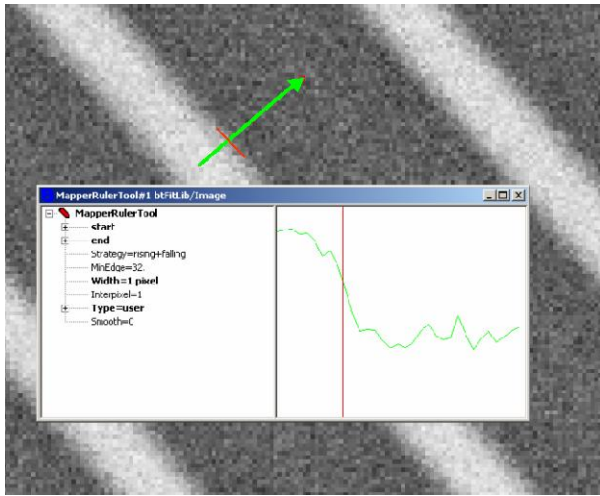


Figure 12. Line edge detection. The steepest slope of the intensity profile defines the edge of the line.

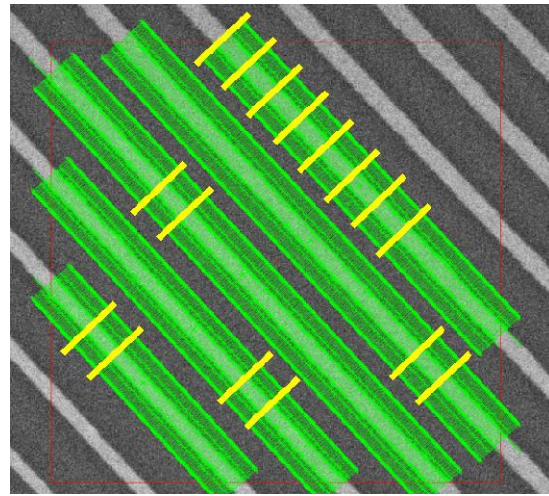


Figure 13. Rulers are placed along the length of the lines. The lines are divided into CD cells, indicated by the yellow bars, of twice the length of the critical dimension.

Figure 12 shows a ruler (the arrow) placed on a line segment within the SEM image. The inset shows the intensity profile along the length of this ruler. The steepest slope of the intensity profile determines the edge of the line, indicated by the vertical line in the inset. Subsequently rulers are placed over the length over the lines, see Figure 13. For each ruler the distance between the found edges is determined. Then the average is taken for all rulers within a line segment of twice the Critical Dimension (CD) of the line, several of these segments are indicated by the bars in Figure 13. Three times the standard deviation of these CD cells within one image is what we call within-beam-CDu.

Resist exposure results

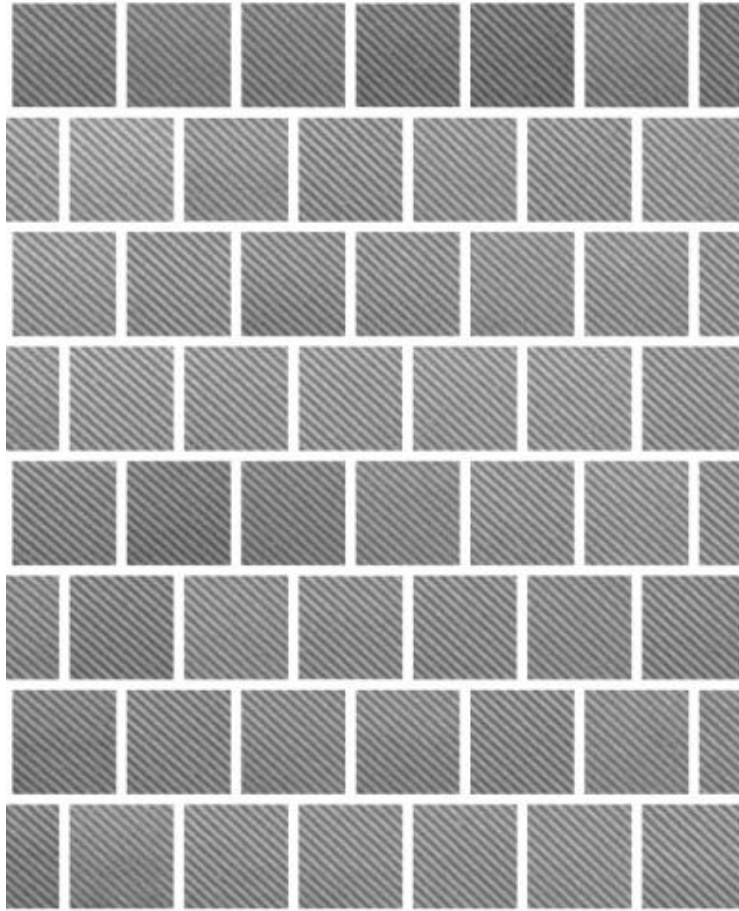


Figure 14. Resist exposure results of 40 nm dense lines performed in the MAPPER Demonstrator.

Resist exposure are done on a bi-layer resist, 40 nm HSQ image layer with a 90 nm photo resist bottom layer. After exposure, the HSQ is developed in TMAH and used as an etch mask in an O₂ reactive-ion etcher. The pattern is transferred onto the photo resist bottom layer. Then for each beamlet a SEM image is made. Again, a 1x1 μm^2 region is cropped from these images and placed on a hexagonal grid to display the result of the exposure in Figure 14. By visual inspection you can already see that each beam gives very similar dense lines patterns.

We have analyzed the SEM images of 65 neighboring beamlets. For each beamlet there were 70 CD cells. The average of these 70 CD cells is the beamlet CD, shown in Figure 15 for each beamlet. Also three times the standard deviation of these 70 CD cells, the within-beam CDu, is shown for each beamlet in Figure 15.

Typical line width variation should be less than 10% of the CD, in this case less than 4 nm. Two types of CDu are analyzed, namely within-beam CDu and beam-to-beam CDu.

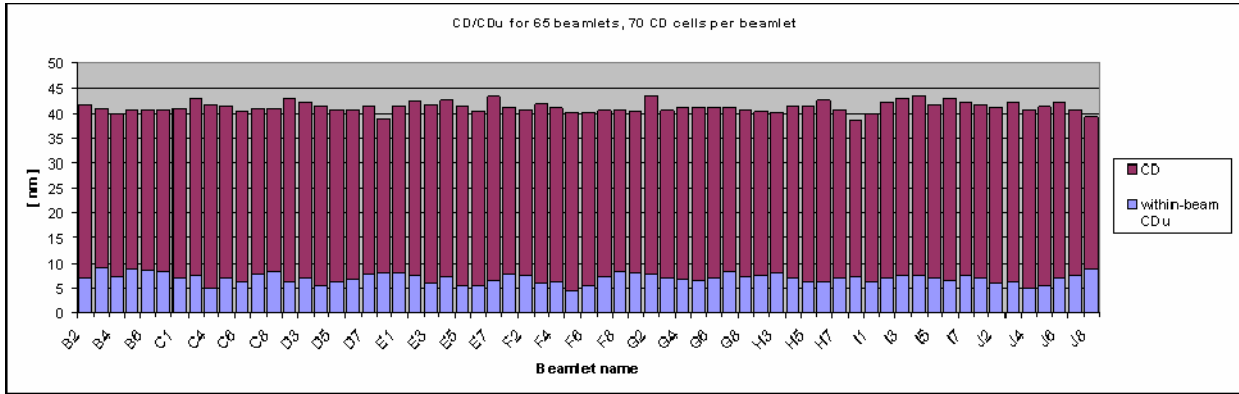


Figure 15. The CD and within-beam CDu for each beamlet.

The beamlet CD ranges from 38.5 nm to 43.6 nm with an average CD of 41.3 nm and three times the standard deviation of 3.2 nm. This means that the beam-to-beam CDu is better than 10% of the CD. Three times the standard deviation of all $65 \cdot 70 = 4550$ CD cells is 7.7 nm, but this includes the within-beam CDu. The average within-beam CDu is 7.0 nm and is somewhat larger than required. This is most likely due to worse exposure latitude than required, i.e. a spot size larger than the required 31 nm.

We have measured the spot sizes of all beamlets and found 45 nm. Using this spot size and the equation for CDu from Ref. [6]:

$$CDu_{IL} = \frac{1}{XL} \cdot 3 \cdot \sqrt{\frac{q_e \cdot \left(1 + \frac{1}{\gamma_1} + \frac{1}{\gamma_1 \gamma_2}\right)}{D \cdot (c_1 \cdot d_r \cdot L_{CDu})}} + \sigma_{dose_other}^2 \quad (1)$$

with XL , the exposure latitude taken from Ref. [6], γ_1 is the fraction of primary electrons that result in secondary electrons that really contribute to the resist exposure and γ_2 is the average number of acids created per secondary electron, D is the exposure dose, L_{CDu} is the resist averaging length and c_1 is a scaling factor of $1.9^{[4]}$. The electron charge is given by q_e .

If we calculate XL with a spot size of 45 nm, use a dose D of $65 \mu\text{C}/\text{cm}^2$, an averaging length L_{CDu} of 90 nm, and typical numbers for γ , we find $CDu_{IL} = 7$ nm. This corresponds very well with the within-beam CDu found for our exposure results.

These results demonstrate that a multi-beam system can meet the requirements for beam-to-beam Critical Dimension Uniformity.

4. CONCLUSIONS

Electron beam lithography is capable of very high resolution down to 10 nm in resist. Its throughput is the main challenge, which can be overcome by the multi-beam MAPPER concept. It requires a high-brightness source, which can deliver a lot of current on the wafer and an optically switched blanker array to individually control the beamlets.

We have presented resist exposures results of a fully functional electron optics column and shown the viability of MAPPER's multi-beam concept. Furthermore, we have shown that a multi-beam electron optics column can meet the requirements for beam-to-beam Critical Dimension Uniformity.

REFERENCES

- [1] A.N. Broers, A.C.F. Hoole, and J.M. Ryan, *Electron beam lithography – Resolution limits*, Micro-Electronic Engineering **32** (1996) 131-142
- [2] N. Silvis-Cividjian *et al.*, *Direct fabrication of nanowires in an electron microscope*, Appl. Phys. Lett. **82** (2003) 3514-3516.
- [3] International Technology Roadmap for Semiconductor, 2007 update, www.itrs.net
- [4] P. Kruit, S. Steenbrink, R. Jager, and M. Wieland, J. Vac. Sci. Technol. B **22**(6), pp 2948-2955 (2004)
- [5] G.H. Jansen, J. Appl. Phys. **84**, pp 4549-4567 (1998)
- [6] S.W.H.K. Steenbrink *et al.*, High Throughput Maskless Lithography: Low Voltage versus High Voltage, Proc Spie **6921** (2008)
- [7] T.F. Teepe *et al.*, J. Vac. Sci. Technol. B **23** (2), 359-369 (2005)
- [8] A.J. van den Brom *et al.*, J. Vac. Sci. Technol. **25** (6), 2245-2249 (2007)
- [9] G. Gärtner *et al.*, Appl. Surf. Sci. **111**, 11-17 (1997)